

Morphology of the earliest reconstructable tetrapod *Parmastega aelidae*

<https://doi.org/10.1038/s41586-019-1636-y>

Pavel A. Beznosov¹, Jennifer A. Clack², Ervins Lukševičs³, Marcello Ruta⁴ & Per Erik Ahlberg^{5*}

Received: 8 April 2019

Accepted: 10 September 2019

Published online: 23 October 2019

The known diversity of tetrapods of the Devonian period has increased markedly in recent decades, but their fossil record consists mostly of tantalizing fragments^{1–15}. The framework for interpreting the morphology and palaeobiology of Devonian tetrapods is dominated by the near complete fossils of *Ichthyostega* and *Acanthostega*; the less complete, but partly reconstructable, *Ventastega* and *Tulerpeton* have supporting roles^{2,4,16–34}. All four of these genera date to the late Famennian age (about 365–359 million years ago)—they are 10 million years younger than the earliest known tetrapod fragments^{5,10}, and nearly 30 million years younger than the oldest known tetrapod footprints³⁵. Here we describe *Parmastega aelidae* gen. et sp. nov., a tetrapod from Russia dated to the earliest Famennian age (about 372 million years ago), represented by three-dimensional material that enables the reconstruction of the skull and shoulder girdle. The raised orbits, lateral line canals and weakly ossified postcranial skeleton of *P. aelidae* suggest a largely aquatic, surface-cruising animal. In Bayesian and parsimony-based phylogenetic analyses, the majority of trees place *Parmastega* as a sister group to all other tetrapods.

The rate of discovery of Devonian tetrapods accelerated greatly during the late twentieth and early twenty-first centuries. The description of *Ichthyostega* in 1932 was followed by *Acanthostega* in 1952, *Metaxygnathus* in 1977 and *Tulerpeton* in 1984; all other descriptions or identifications of genera (*Hynierpeton*, *Ventastega*, *Elginerpeton*, *Obruchevichthys*, *Densignathus*, *Sinostega*, *Jakubsonia*, *Ymeria*, *Webererpeton*, *Tutusius* and *Umzantsia*) as Devonian tetrapods have occurred since 1994^{1–11,16,17}. Unnamed Devonian tetrapod material has previously been described from Belgium^{12,13} and the USA^{14,15}. However, the fossils of *Ichthyostega* and *Acanthostega* from East Greenland^{9,16–31} remain by far the most complete material for Devonian tetrapods, followed by *Ventastega* fossils from Latvia^{4,31,32} and *Tulerpeton* fossils from Russia^{2,33,34}. All of these date to the final stage of the Devonian period (the late Famennian), by which point tetrapods had been in existence for about 30 million years (judging by evidence from trackways^{35,36}) and had colonized both equatorial and polar environments¹¹. Substantial differences between these four genera hint at long, divergent evolutionary histories; notably, the *Ichthyostega* and *Acanthostega* fossils have braincases that are fundamentally dissimilar to each other²⁰.

The tetrapod material described here is securely dated to the earliest Famennian age, and is comparable to that of *Ventastega* in its degree of completeness. It is derived from the Sosnogorsk Formation of the southern part of Timan Ridge (Komi Republic, Russia)³⁷, which straddles the boundary between the Frasnian age (about 382–372 million years ago) and the Famennian age; vertebrate remains occur only in the part of the Sosnogorsk Formation that dates to the Famennian age (Extended Data Fig. 1). The material described here is thus only marginally younger than the oldest known tetrapods *Elginerpeton*, *Obruchevichthys* and *Webererpeton*, which are known only from fragmentary material^{5,10}.

The quality of the material described here, which consists of numerous isolated bones and some articulated skull regions, is excellent. Multiple examples of the same bone all show the same distinctive features (Extended Data Fig. 2), which indicates that only a single tetrapod species is present (Extended Data Fig. 3). These fossils give a detailed picture of an animal from the earliest part of the known body-fossil record of the tetrapods.

Systematic palaeontology

Tetrapoda Jaekel, 1909
Parmastega aelidae gen. et sp. nov.

Remarks. The term Tetrapoda is used here in its traditional, apomorphy-based sense of limbed vertebrates.

Etymology. The generic name derives from *parma*, a word in the Komi language describing the landscape of hills covered by coniferous forest, typical for South Timan, and *stégi* (Greek) meaning roof, understood here as the skull roof; *aelidae* honours Aelida I. Popova (Syktyvkar State University) (1929–2011), who first inspired P.A.B.'s interest in the natural sciences.

Holotype. Institute of Geology, Komi Science Centre (IG KSC) 705/1, an articulated snout region (Fig. 1a–c).

Referred material. One hundred and six individual bones or bone assemblies (Supplementary Table 1).

¹Institute of Geology, Komi Science Centre, Ural Branch of the Russian Academy of Sciences, Syktyvkar, Russia. ²University Museum of Zoology, University of Cambridge, Cambridge, UK.

³Department of Geology, University of Latvia, Riga, Latvia. ⁴Joseph Banks Laboratories, School of Life Sciences, University of Lincoln, Lincoln, UK. ⁵Department of Organismal Biology, Uppsala University, Uppsala, Sweden. *e-mail: per.ahlberg@ebc.uu.se

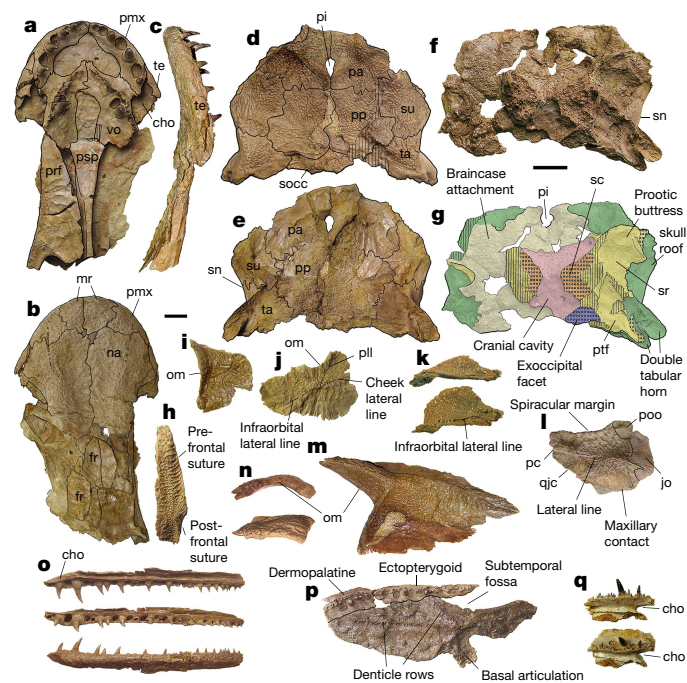


Fig. 1 | Skull roof, cheek and palate of *P. aelidae*. **a–c**, Specimen IGKSC 705/1 (all numerical codes in the figure legends refer to specimen numbers in the IGKSC collections), the holotype of *P. aelidae*. Articulated ethmosphenoid with associated prefrontal in ventral (**a**), dorsal (**b**) and lateral (**c**) views. **d, e**, 705/2. Skull table in dorsal (**d**) and ventral (**e**) views. **f, g**, 705/17. Skull table and partial braincase in ventral view. **g**, False-colour image identifying the components of 705/17. **h**, 705/18. Right frontal, external view. **i, j**, 705/19. Left postorbital, external view. **j**, 705/20. Left jugal, external view. **k**, 705/25. Left lacrimal, lateral (top) and dorsal (bottom) views. **l**, 705/26. Right squamosal, external view. **m**, 705/5. Right prefrontal, external view. **n**, 705/4. Left postfrontal, lateral (top) and dorsal (bottom) views. **o**, 705/28. Right maxilla in internal (top), ventral (middle) and external (bottom) views. **p**, 705/29 (left dermopalatine), 705/30 (ectopterygoid) and 705/31 (pterygoid) in ventral view. **q**, 705/32. Left dermopalatine in lateral (top) and ventral (bottom) views. cho, choana; fr, frontal; jo, jugal overlap; mr, median rostrals; na, nasal; om, orbital margin; pa, parietal; pc, preopercular contact; pi, pineal foramen; pmx, premaxilla; pll, postorbital lateral line; poo, postorbital overlap; pp, postparietal; prf, prefrontal; psp, parasphenoid; ptf, posttemporal fossa; qjc, quadratojugal contact; sc, semicircular canals; socc, supraoccipital; sn, spiracular notch; sr, spiracular recess; su, supratemporal; ta, tabular; te, tectal; vo, vomer. Scale bars, 10 mm (scale bar below **f** applies to **f, g**; the scale bar below **c** applies to all other panels).

Locality and horizon. Sosnovskiy Geological Monument, on the right bank of the Izhma River opposite Sosnogorsk (Komi Republic, Russia); Sosnogorsk Formation, lowermost Famennian age (Extended Data Fig. 1).

Diagnosis. A stem tetrapod diagnosed by the following unique combination of characters: dermal ornament of preorbital region developed into transverse parallel 'wave crests' with a spacing of a few millimetres; ornament present on dorsal blade of cleithrum and on anocleithrum; orbit strongly raised above skull roof, framed by an anterodorsal crest and a vertical anterior ridge carried on prefrontal; internasal fontanelle absent; median rostral paired; lacrimal excluded from orbit by prefrontal–jugal contact; intertemporal absent; pterygoids separated in midline by parasphenoid; interpterygoid vacuities absent; pterygoid dentition restricted to two lines of denticles, running anteriorly and anterolaterally from growth centre; ectopterygoid making large contribution to lateral wall of subtemporal fossa; middle part of otic capsule narrow, occupying approximately half of skull table width; posttemporal fossa wide, triangular; fang pair and row of marginal teeth on adsymphysial

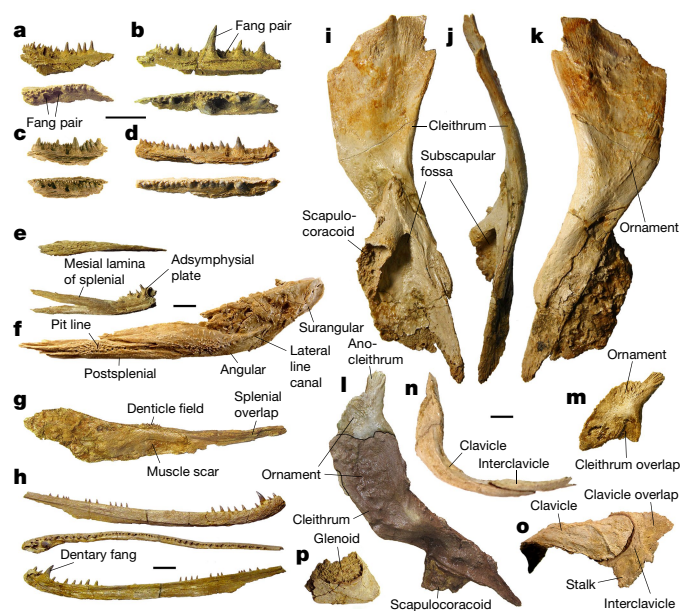


Fig. 2 | Lower jaw and pectoral girdle of *P. aelidae*. **a**, 705/21. Right adsymphysial plate in mesial (top) and dorsal (bottom) views. **b**, 705/22. Right anterior coronoid in mesial (top) and dorsal (bottom) views. **c**, 705/33. Right middle coronoid in mesial (top) and dorsal (bottom) views. **d**, 705/36. Left posterior coronoid in mesial (top) and dorsal (bottom) views. **e**, 705/37. Articulated left splenial and adsymphysial plate in ventrolateral (top) and mesial (bottom) views. **f**, 705/34. Articulated left postsplenial, angular and surangular in lateral view. **g**, 705/76. Left prearticular in mesial view. **h**, 705/67. Right dentary in lateral (top), dorsal (middle) and mesial (bottom) views. **i–k**, 705/15. Left cleithrum and partial scapulocoracoid in mesial (**i**), anterior (**j**) and lateral (**k**) views. **l**, 705/95 (right cleithrum) and 705/98 (anocleithrum) in lateral view. **m**, 705/98. Right anocleithrum in lateral view. **n–o**, 705/92 (right clavicle) and 705/89 (interclavicle) in anterior (**n**) and ventral (**o**) views. **p**, 705/102. Left coracoid in lateral view. Scale bars, 10 mm (scale bar between **a–d** applies to these four panels; **e–p** are all shown at the same scale).

plate; middle part of prearticular with large muscle scar; interclavicle rounded with short posterior process.

Description

The *Parmastega* material comprises the entire dermal skull (apart from the preopercular and the posterior part of the quadratojugal), the entire ethmoid and dorsal part of the otoccipital braincase, the entire lower jaw, the dermal pectoral girdle and the partly ossified scapulocoracoid (Figs. 1, 2). The material consists of a total of 106 numbered specimens (Supplementary Tables 1, 2), which represents a minimum of 11 individuals; these individuals show a wide range of sizes (Extended Data Figs. 2, 4), but were found within a small area of the site (Extended Data Fig. 1). Most specimens are isolated bones, but an articulated ethmoid (Fig. 1a–c) and several skull tables (Fig. 1d–g) are also present. The bones are three-dimensionally preserved in limestone with little or no distortion, and have been freed from the matrix using dilute acetic acid (Methods). Bones from the same individual can sometimes be identified by matching size and sutural fit (Extended Data Fig. 3). This allows us to reconstruct the skull, lower jaw and pectoral girdle with a high degree of confidence, except for the posterior part of the suspensorium (Fig. 3). Assuming proportions similar to those of *Acanthostega*¹⁹, the maximum length of *Parmastega* was approximately 130 cm.

The shape of the skull is broadly similar to that of *Ventastega* and *Acanthostega*, although the orbits of *Parmastega* are raised higher above the skull table and the snout has a distinctly concave profile (Extended Data Fig. 4). The strongly raised orbits and relatively narrow snout are

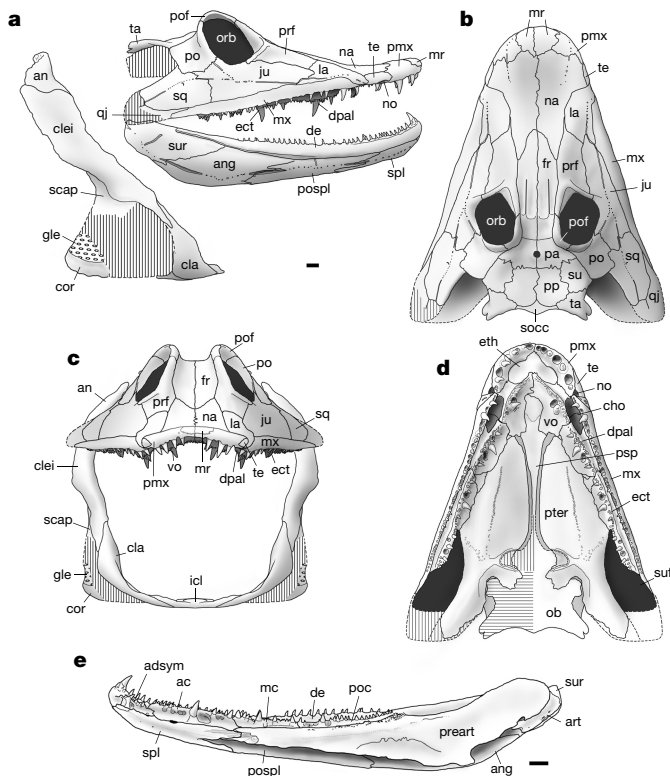


Fig. 3 | Reconstructions of *P. aelidae*. **a**, Skull, lower jaw and pectoral girdle of *Parmastega* in right lateral view. **b**, Skull in dorsal view. **c**, Skull and pectoral girdle in anterior view. **d**, Skull in ventral view. **e**, Right lower jaw ramus in mesial view. ac, anterior coronoid; adsym, adsymphyseal plate; an, anocleithrum; ang, angular; art, articular; cla, clavicle; clei, cleithrum; cor, coracoid; de, dentary; dpal, dermopalatine; ect, ectopterygoid; eth, ethmoid; gle, glenoid; icl, interclavicle; ju, jugal; la, lacrimal; mc, middle coronoid; mx, maxilla; no, nostril; orb, orbit; ob, otoccipital braincase; po, postorbital; poc, posterior coronoid; pof, postfrontal; pospl, postsplenial; preart, prearticular; pter, pterygoid; qj, quadratojugal; scap, scapula; spl, splenial; sq, squamosal; suf, subtemporal fossa; sur, surangular. Vertical hatching indicates a missing element with unknown outline; horizontal hatching indicates a damaged object with known outline. Scale of reconstruction determined by largest individual. Scale bars, 10 mm (**a–d** are all shown to the same scale, which is given in **a**).

reminiscent of the elpistostegids *Elpistostege* and *Tiktaalik*^{38,39}. However, the orbits of *Parmastega* are proportionately larger than those in the elpistostegids (Extended Data Fig. 5).

The dermal bone pattern of the skull roof and cheeks is, with a single exception, characteristic of Devonian tetrapods. There is no postrostral mosaic or internasal fontanelle. The median rostral is paired as in *Acanthostega*, *Ventastega* and *Elpistostege*, but unlike in *Ichthyostega* and *Elginerpeton* in which it is single^{5,18,26,32,38}. A tectal bone forms the dorsal margin of the naris, which lies very close to the jaw margin and faces ventrally; the ventral margin of the naris is formed by the maxilla, as there is no lateral rostral. The lacrimal is excluded from the orbit by a long suture between the jugal and prefrontal. The latter is elongate and carries two bony crests, one forming the anterior part of the ‘eyebrow’ and the other an oblique ridge in front of the orbit; both are more strongly developed in large specimens (Figs. 1m, 3a–c). The frontals are elongate with a distinct transverse ‘step’ on the posterior part of the dorsal surface, marking the transition from snout to skull table. Intertemporals are absent. The lateral margins of the supratemporal and tabular form a raised spiracular margin; the tabular horn has distinct dorsal and ventral components. A small part of the dorsal surface of the braincase is exposed posterior to the tabulars. The dermal ornament

of the preorbital region includes areas of irregular transverse ripples (Fig. 1h, m, Extended Data Fig. 2), somewhat similar to the ornament of *Umzantsia*¹¹ but much coarser; elsewhere, the ornament grades into the conventional tetrapod ‘starburst’ ornament. Partly enclosed sensory-line canals are well-developed on the premaxilla, cheek bones and the anterior part of the nasals, but are absent from the skull table (Fig. 1d).

Between the anterior suture for the jugal and the posterior suture for the preopercular, the ventral margin of the squamosal presents two distinct sutural margins that appear to be contacts for two bones (Fig. 1l). The posterior of these margins must be for the quadratojugal; as the jugal lacks a posterior process, we tentatively infer that the anterior segment of the ventral margin of the squamosal contacts the maxilla (Fig. 3a). A squamosal–maxillary contact is characteristic for ‘fish’ members of the tetrapod stem-group (such as *Eusthenopteron*⁴⁰) and its presence in *Parmastega* is unique among tetrapods.

The palatal morphology of *Parmastega* is intermediate between that of the elpistostegids and that of Devonian tetrapods. In the elpistostegids *Panderichthys* and *Tiktaalik*, the pterygoids are separated in the midline by a long denticulated parasphenoid^{41,42}. The vomer has a transverse posterior margin; in *Panderichthys*, this margin ends mesially in a short posterior process that extends along the lateral margin of the parasphenoid⁴¹. This condition is broadly similar to that observed in *Eusthenopteron*⁴⁰. By contrast, in *Ichthyostega*, *Acanthostega* and *Ventastega*, the pterygoids meet in the midline (separating the parasphenoid from the vomer) and the most-posterior point of the vomer is its posterolateral corner^{4,18,23}. In *Parmastega*, the parasphenoid separates the pterygoids but is not denticulated anteriorly, and the vomeral morphology is intermediate between that of *Panderichthys* and Devonian tetrapods (Figs. 1a, 3d). The pterygoid carries a longitudinal row or narrow band of denticles, and a shorter oblique band that extends anterolaterally. Uniquely, the ectopterygoid extends posteriorly past its contact with the pterygoid to contribute to the lateral margin of the subtemporal fossa (Fig. 3d). This relationship is demonstrated by a sutural fit of three bones from one individual (Fig. 1p).

Two parts of the braincase are preserved: the ethmoid and part of the sphenoid in IG KSC 705/1, and the dorsal part of the otoccipital in IG KSC 705/17 (Fig. 1a, f, g). An ossified ethmoid is shared only with *Ichthyostega* among known Devonian tetrapods³⁸. The otoccipital has a strongly developed pro-otic buttress, a narrow cranial cavity with small inner ears and a posttemporal fossa that is bounded laterally by a crista parotica that extends onto the tabular horn. In ventral view, the outline of the occipital resembles that of *Tiktaalik*⁴², but is proportionately broader in *Parmastega*. Otoccipitals that are previously known from Devonian tetrapods show one of two radically different morphologies. In *Acanthostega* and *Ventastega*, the narrow posttemporal fossa is open laterally and the braincase occupies almost the whole ventral surface of the skull table; by contrast, the narrow braincase in *Ichthyostega* is flanked by large cavities under the skull table that probably housed spiracular diverticula^{20,24,25,32}. The otoccipital of *Parmastega* provides a plausible ancestral groundplan for both of these morphologies (Extended Data Fig. 6).

The construction of the lower jaw is typical for tetrapods³⁰, although it is unusually slender and delicate (Figs. 2a–h, 3e). The only ossified parts of the Meckelian element are the articular and the symphysis. The prearticular carries very few denticles but bears a large ventral muscle scar on its middle part. The contact between the prearticular and the mesial lamina of the splenial is not a tight suture, as in other known Devonian tetrapods³⁰, but is instead a loose overlap that must have contained a ligamentous component and allowed a degree of flexibility. Fang pairs—positioned mesial to the tooth row—are present on the adsymphyseal plate, dentary, and anterior and middle coronoids. Postsplenial and surangular pit lines are present. The dentary is splint-like and loosely attached.

The pectoral girdle is U-shaped in anterior view, and the dorsal blades of the cleithra are approximately parallel (Figs. 2i–o, 3a, c). The dorsal orientation of the anocleithrum, which we determined from well-preserved

contact surfaces, makes the girdle notably tall. The cleithrum and anocleithrum both carry a dermal ornament, a characteristic that is otherwise absent in known tetrapods (except for *Umzantsia*¹¹). The clavicle is narrow, and the interclavicle has a rounded corpus with a short posterior process (Fig. 2n, o); both of these bones somewhat resemble the corresponding elements in *Ichthyostega*¹⁸, whereas *Acanthostega* and *Ventastega* have broader clavicles and lozenge-shaped interclavicles^{29,32}. The scapulocoracoid is ossified in two parts: a dorsal scapular part that is co-ossified with the cleithrum (Fig. 2i) and a posterior coracoid ossification that carries the glenoid (Fig. 2p). As in *Ichthyostega*, *Elginerpeton* and *Hynerpeton*, the subscapular fossa is deep and has a narrow apex; by contrast, in *Acanthostega* and *Ventastega* the fossa is shallow and broad^{3,18,29,32,43}. The limbs, pelvis, vertebrae and ribs are not preserved in the material from Sosnogorsk.

Phylogenetic analysis

We evaluated the phylogenetic position of *Parmastega* with maximum parsimony and Bayesian inference analyses, applied to a data matrix of 26 taxa and 113 characters (Methods). The character list and data matrix are provided in the Supplementary Information.

The resolution of the strict-consensus, unweighted parsimony analysis was poor: all of the Devonian tetrapods (including *Parmastega*) formed a polytomy together with ‘whatcheeriid-grade’ Carboniferous taxa (Extended Data Fig. 7a). However, in 70% of the trees, *Parmastega* was the sister group to all other tetrapods. We used a range of approaches (character reweighting by rescaled consistency index and *K* values, and the calculation of agreement subtrees from consensus trees) to investigate the phylogenetic signal in the dataset (Extended Data Fig. 7b, c, e–h), which revealed consistent patterns. If the position of *Parmastega* was resolved, it was always placed as the sister group to all other tetrapods; if *Ventastega* was resolved, it was placed immediately crownward of *Parmastega*. *Ichthyostega* was resolved crownward of *Acanthostega* in the Adams consensus of unweighted trees, but in the reweighted analyses *Acanthostega* was crownward of *Ichthyostega*. The Bayesian tree (Extended Data Fig. 7d) also recovered these positions for *Parmastega* and *Ventastega*, but did not resolve *Ichthyostega* and *Acanthostega*.

Discussion

Parmastega is morphologically intermediate between the elpistostegids *Tiktaalik*, *Elpistostege* and *Panderichthys* on the one hand, and previously known Devonian tetrapods on the other—but primitive and derived characters are not evenly distributed across its anatomy. The lower jaw, pectoral girdle, external dermal bone pattern of the snout region, the absence of gular plates and the relative size of the orbits are all tetrapod-like, whereas elpistostegid-like characteristics persist in the palate and the dermal ornamentation of the cleithrum and anocleithrum. Although no appendage bones are known, the morphology of the pectoral girdle strongly suggests that *Parmastega* possessed limbs rather than paired fins. The scapulocoracoid, which forms the proximal attachment for many forelimb muscles and undergoes substantial changes in shape from elpistostegids^{44,45} to tetrapods^{3,18,29,32,34}, is particularly informative in this regard: *Parmastega* conforms to the tetrapod pattern. The shape and construction of the lower jaw, and the absence of gular plates, suggest that gill ventilation and prey capture worked in the same way as in more-crownward Devonian tetrapods. The reconfiguration of the palate and the loss of dermal ornament on the shoulder girdle evidently lagged behind these transformations.

Until now, one of the most puzzling aspects of the anatomy of Devonian tetrapods has been the specialized ear region of *Ichthyostega*, which differs markedly from the ear regions in other early tetrapods^{18,20}. The braincase of *Parmastega* is morphologically intermediate between that of *Ichthyostega* and those of *Acanthostega* and *Ventastega*, providing

a plausible hypothetical ancestor for both patterns (Extended Data Fig. 6a). However, these transformations cannot be mapped parsimoniously onto the phylogeny, indicating the presence of non-trivial homoplasy either in the braincases or in other parts of the skeleton (Extended Data Fig. 6b).

The three-dimensional preservation and apparent absence of post-mortem transport makes the *Parmastega* fossils palaeobiologically informative. The environment of preservation, which was probably also the living environment of *Parmastega*, was a coastal lagoon with brackish water and a rich fish fauna including the placoderm *Bothriolepis* and various sarcopterygians⁴⁶. The concentration of the tetrapod remains in a small area of the site (Extended Data Fig. 1) suggests that *Parmastega* may have been a schooling animal. The vertebrate-bearing bed (bed 40, the ‘fish dolomite’) is composed of two consecutive tempestites; possibly a school of *Parmastega* was killed by the first storm event and their skeletons partly disarticulated by the second. Schooling behaviour is also implied by the mass occurrence of *Acanthostega* on Stensiö Bjerg (East Greenland)⁴⁷.

Raised orbits and a lack of lateral line canals on the skull table in *Parmastega* (Fig. 3a, b) suggests it adopted a surface-skimming position in the water, with emergent eyes, similar to that of extant crocodylians (Extended Data Fig. 8). The increase in orbit size across the transition between fish and tetrapods has previously been linked to a shift from aquatic to aerial vision⁴⁸; the relative orbit size of *Parmastega* falls well within the tetrapod range (Extended Data Fig. 5) and its eyes were thus probably adapted for use in air. Although all known Devonian tetrapods have dorsally positioned eyes, *Parmastega* shows the most extreme condition (Extended Data Fig. 4). The nostrils of *Parmastega* face ventrally, which suggests that the nose was not used for breathing air (Extended Data Fig. 8). The dorsally placed spiracles may have taken on this function, as has previously been argued for *Panderichthys*⁴⁹ and more-crownward Devonian tetrapods^{20,22}. Similar to the condition in *Ventastega*, *Acanthostega*³¹ and *Ichthyostega*¹⁸, the lower jaw does not match the upper jaw in curvature in lateral or in ventral view (Extended Data Fig. 9).

The *Parmastega* material contains no vertebrae, ribs, pelvic girdles or limb bones. The lack of evidence for post-mortem transport, the partially ossified nature of the scapulocoracoid even in the largest individuals and the preservation of the delicate isolated coracoid ossifications (Fig. 2i–l, p) suggest that this absence is not a taphonomic artefact but that it instead reflects a very lightly ossified, or even cartilaginous, axial and appendicular skeleton. *Ventastega* may also have had a lightly ossified postcranial skeleton³². *Acanthostega* and *Ichthyostega* became fully ossified as adults^{17–19,21,27,29}, but *Acanthostega* appears to have had a long juvenile stage with non-ossified endoskeleton⁴⁷. Functionally, the poor ossification of *Parmastega* suggests little or no capacity for terrestrial locomotion. This contrasts strangely with the cranial morphology, which suggests that the eyes were habitually held above the surface of the water—and thus implies some kind of engagement with the terrestrial environment. Even more puzzling is the fact that this poorly ossified postcranial skeleton is apomorphic: elpistostegids are well-ossified, as are the majority of tetrapodomorph fishes^{39,40,45}.

Parmastega gives us the earliest detailed glimpse of a tetrapod: an aquatic, surface-skimming predator, just over a metre in length, living in a lagoon on a tropical coastal plain. *Parmastega* is phylogenetically the least-crownward of all of the non-fragmentary tetrapods, but it is not necessarily representative of the primitive conditions for the group. The slightly earlier *Elginerpeton*—which was also probably aquatic and was even larger than *Parmastega* (Extended Data Fig. 4)—had well-ossified girdles and limb bones, as well as a distinctive head shape with a narrow snout^{5,30,43}. Moreover, the trackway record shows that tetrapods originated at least 20 million years before *Parmastega*^{35,36}, and the very existence of the trackways—which implies weight-bearing limbs, even if the prints were made in water—points to these forms having well-ossified postcranial skeletons. Together with the evidence for considerable

morphological homoplasy among Devonian tetrapods, this hints at a tangled and still-unknown early history for limbed vertebrates.

Online content

Any methods, additional references, Nature Research reporting summaries, source data, extended data, supplementary information, acknowledgements, peer review information; details of author contributions and competing interests; and statements of data and code availability are available at <https://doi.org/10.1038/s41586-019-1636-y>.

- Campbell, K. S. W. & Bell, M. W. A primitive amphibian from the Late Devonian of New South Wales. *Alcheringa* **1**, 369–381 (1977).
- Lebedev, O. A. The first find of a Devonian tetrapod in USSR [in Russian]. *Doklady Acad. Nauk SSSR* **278**, 1470–1473 (1984).
- Daeschler, E. B., Shubin, N. H., Thomson, K. S. & Amaral, W. W. A Devonian tetrapod from North America. *Science* **265**, 639–642 (1994).
- Ahlberg, P. E., Lukševičs, E. & Lebedev, O. The first tetrapod finds from the Devonian (Upper Famennian) of Latvia. *Phil. Trans. R. Soc. Lond. B* **343**, 303–328 (1994).
- Ahlberg, P. E. *Elginerpeton pancheni* and the earliest tetrapod clade. *Nature* **373**, 420–425 (1995).
- Daeschler, E. B. Early tetrapod jaws from the Late Devonian of Pennsylvania, USA. *J. Paleontol.* **74**, 301–308 (2000).
- Zhu, M., Ahlberg, P. E., Zhao, W. & Jia, L. First Devonian tetrapod from Asia. *Nature* **420**, 760–761 (2002).
- Lebedev, O. A. A new tetrapod *Jakubsonia livnensis* from the Early Famennian (Devonian) of Russia and palaeoecological remarks on the Late Devonian tetrapod habitats. *Acta Univ. Latviensis* **679**, 79–98 (2004).
- Clack, J. A., Ahlberg, P. E., Blom, H. & Finney, S. M. A new genus of Devonian tetrapod from North-East Greenland, with new information on the lower jaw of *Ichthyostega*. *Palaeontology* **55**, 73–86 (2012).
- Clément, G. et al. Devonian tetrapod from western Europe. *Nature* **427**, 412–413 (2004).
- Olive, S. et al. New discoveries of tetrapods (ichthyostegid-like and whatcheeriid-like) in the Famennian (Late Devonian) localities of Strud and Becco (Belgium). *Palaeontology* **59**, 827–840 (2016).
- Shubin, N. H., Daeschler, E. B. & Coates, M. I. The early evolution of the tetrapod humerus. *Science* **304**, 90–93 (2004).
- Daeschler, E. B., Clack, J. A. & Shubin, N. H. Late Devonian tetrapod remains from Red Hill, Pennsylvania, USA: how much diversity? *Acta Zool.* **90**, 306–317 (2009).
- Säve-Söderbergh, G. Preliminary note on Devonian stegocephalians from East Greenland. *Medd. Grönl.* **94**, 1–107 (1932).
- Jarvik, E. On the fish-like tail in the ichthyostegid stegocephalians with descriptions of a new stegocephalian and a new crossopterygian from the Upper Devonian of East Greenland. *Medd. Grönl.* **114**, 1–90 (1952).
- Jarvik, E. *The Devonian Tetrapod Ichthyostega (Fossils & Strata no. 40)* (Scandinavian Univ. Press, 1996).
- Ahlberg, P. E., Clack, J. A. & Blom, H. The axial skeleton of the Devonian tetrapod *Ichthyostega*. *Nature* **437**, 137–140 (2005).
- Clack, J. A. et al. A uniquely specialized ear in a very early tetrapod. *Nature* **425**, 65–69 (2003).
- Callier, V., Clack, J. A. & Ahlberg, P. E. Contrasting developmental trajectories in the earliest known tetrapod forelimbs. *Science* **324**, 364–367 (2009).
- Clack, J. A. Discovery of the earliest-known tetrapod stapes. *Nature* **342**, 425–427 (1989).
- Clack, J. A. *Acanthostega gunnari*, a Devonian tetrapod from Greenland: the snout, palate and ventral parts of the braincase. *Medd. Grönl. Geosci.* **31**, 1–24 (1994).
- Clack, J. A. Earliest known tetrapod braincase and the evolution of the stapes and fenestra ovalis. *Nature* **369**, 392–394 (1994).
- Clack, J. A. The neurocranium of *Acanthostega gunnari* Jarvik and the evolution of the otic region in tetrapods. *Zool. J. Linn. Soc.* **122**, 61–97 (1998).
- Clack, J. A. A revised reconstruction of the dermal skull roof of *Acanthostega gunnari*, an early tetrapod from the Late Devonian. *Trans. R. Soc. Edinb. Earth Sci.* **93**, 163–165 (2002).
- Coates, M. I. & Clack, J. A. Polydactyly in the earliest known tetrapod limbs. *Nature* **347**, 66–69 (1990).
- Coates, M. I. & Clack, J. A. Fish-like gills and breathing in the earliest known tetrapod. *Nature* **352**, 234–236 (1991).
- Coates, M. I. The Devonian tetrapod *Acanthostega gunnari* Jarvik: postcranial anatomy, basal tetrapod interrelationships and patterns of skeletal evolution. *Trans. R. Soc. Edinb. Earth Sci.* **87**, 363–421 (1996).
- Ahlberg, P. E. & Clack, J. A. Lower jaws, lower tetrapods – a review based on the Devonian genus *Acanthostega*. *Trans. R. Soc. Edinb. Earth Sci.* **89**, 11–46 (1998).
- Porro, L. B., Rayfield, E. J. & Clack, J. A. Descriptive anatomy and three-dimensional reconstruction of the skull of the early tetrapod *Acanthostega gunnari* Jarvik, 1952. *PLoS ONE* **10**, e0118882 (2015).
- Ahlberg, P. E., Clack, J. A., Lukševičs, E., Blom, H. & Zupins, I. *Ventastega curonica* and the origin of tetrapod morphology. *Nature* **453**, 1199–1204 (2008).
- Lebedev, O. A. & Clack, J. A. Upper Devonian tetrapods from Andreyevka, Tula Region, Russia. *Palaeontology* **36**, 721–734 (1993).
- Lebedev, O. A. & Coates, M. I. The postcranial skeleton of the Devonian tetrapod *Tulerpeton curtum*. *Zool. J. Linn. Soc.* **114**, 307–348 (1995).
- Niedźwiedzki, G., Szrek, P., Narkiewicz, K., Narkiewicz, M. & Ahlberg, P. E. Tetrapod trackways from the early Middle Devonian period of Poland. *Nature* **463**, 43–48 (2010).
- Stössel, I., Williams, E. A. & Higgs, K. T. Ichthyology and depositional environment of the Middle Devonian Valentia Island tetrapod trackways, south-west Ireland. *Palaeogeogr. Palaeoclimatol. Palaeoecol.* **462**, 16–40 (2016).
- Beznosov, P. Sosnogorsk Formation – a new local stratigraphic unit of the Upper Devonian from South Timan [in Russian]. *Geologiya i mineralnye resursy evropeyskogo servero-vostoka Rossii: materialy XV geologicheskogo s'yezda Respubliki Komi* **2**, 9–12 (2009).
- Schultze, H.-P. & Arsenault, M. The panderichthyid fish *Elpistostege*: a close relative of tetrapods? *Palaeontology* **28**, 293–310 (1985).
- Daeschler, E. B., Shubin, N. H. & Jenkins, F. A. Jr. A Devonian tetrapod-like fish and the evolution of the tetrapod body plan. *Nature* **440**, 757–763 (2006).
- Jarvik, E. *Basic Structure and Evolution of Vertebrates* Vol. 1 (Academic, 1980).
- Ahlberg, P. E., Clack, J. A. & Lukševičs, E. Rapid braincase evolution between *Panderichthys* and the earliest tetrapods. *Nature* **381**, 61–64 (1996).
- Downs, J. P., Daeschler, E. B., Jenkins, F. A. Jr & Shubin, N. H. The cranial endoskeleton of *Tiktaalik roseae*. *Nature* **455**, 925–929 (2008).
- Ahlberg, P. E. Postcranial stem tetrapod remains from the Devonian of Scat Craig, Morayshire, Scotland. *Zool. J. Linn. Soc.* **122**, 99–141 (1998).
- Vorobyeva, E. I. The shoulder girdle of *Panderichthys rhombolepis* (Gross) (Crossopterygii); Upper Devonian; Latvia. *Geobios* **28**, 285–288 (1995).
- Shubin, N. H., Daeschler, E. B. & Jenkins, F. A. Jr. The pectoral fin of *Tiktaalik roseae* and the origin of the tetrapod limb. *Nature* **440**, 764–771 (2006).
- Lukševičs, E., Beznosov, P. & Stūris, V. A new assessment of the Late Devonian antiarchan fish *Bothriolepis leptocheira* from South Timan (Russia) and the biotic crisis near the Frasnian–Famennian boundary. *Acta Paleontol. Pol.* **62**, 97–119 (2017).
- Sanchez, S., Tafforeau, P., Clack, J. A. & Ahlberg, P. E. Life history of the stem tetrapod *Acanthostega* revealed by synchrotron microtomography. *Nature* **537**, 408–411 (2016).
- Maclver, M. A., Schmitz, L., Mugaň, U., Murphey, T. D. & Mobley, C. D. Massive increase in visual range preceded the origin of terrestrial vertebrates. *Proc. Natl Acad. Sci. USA* **114**, E2375–E2384 (2017).
- Brazeau, M. D. & Ahlberg, P. E. Tetrapod-like middle ear architecture in a Devonian fish. *Nature* **439**, 318–321 (2006).

Publisher's note Springer Nature remains neutral with regard to jurisdictional claims in published maps and institutional affiliations.

© The Author(s), under exclusive licence to Springer Nature Limited 2019

Methods

Preparation and illustration of specimens

The specimens were collected from the Sosnovskiy Geological Monument, on the right bank of the river Izhma opposite Sosnogorsk Town (Komi Republic, Russia), during a series of field seasons from 2002 to 2012. The bulk of the material was collected during a large-scale excavation in 2009–2012, during which approximately 50 m² of the bone-bearing ‘fish dolomite’ bed was dug out and then broken into small blocks using hammers, chisels, an angle grinder, drill and portable jackhammer. Blocks that contained parts of the same bone were glued together. The bones were freed from the limestone matrix using dilute (7–10%) acetic acid, alternating with drying and covering with the consolidants PVB (before 2010) and paraloid B-72 (after 2010). The reconstructions of the skull and lower jaw were assembled by hand on the basis of photographs of individual bones, taken at appropriate angles. The reconstruction of the pectoral girdle was produced by sticking together the right anocleithrum, cleithrum, clavicle and interclavicle of one individual, making a three-dimensional virtual model of the assembly using photogrammetry (Agisoft PhotoScan), and importing this model into 3-matic (Materialise), in which it was duplicated, mirrored and assembled into a complete girdle. The drawings of the girdle in Fig. 3 were traced directly from lateral and anterior projections of the model.

Phylogenetic analysis

The phylogenetic position of *Parmastega* was evaluated with maximum parsimony and Bayesian-inference analyses applied to a data matrix of 26 taxa and 113 characters (Supplementary Information), on the basis of a recently published matrix⁵⁰ with the addition of four characters (character numbers 7, 27, 28 and 29). Before all analyses, we explored the occurrence of possible ‘taxonomic equivalents’⁵¹ by subjecting the matrix to safe taxonomic reduction using the Claddis package⁵² in the R environment for statistical computing and graphics (<https://cran.r-project.org>). No taxon was identified as being suitable for safe deletion.

For all parsimony analyses, we used PAUP* version 4.0a (build 164)⁵³ with the following search settings. The ‘collapse branch’ option was enforced for branches that could possibly attain a minimum length of zero. Tree searches used a heuristic option with a tree bisection–reconnection branch-swapping algorithm, and saving no more than a single tree of length greater than or equal to 1 step in each replicate, and using a maximum of 5,000 random step-wise taxon addition replicates while holding a single tree in memory at each step. Following this initial round of tree searches, an additional branch-swapping round was conducted on all trees saved in the memory—this time with the option of saving multiple trees in effect. This second round of tree searches was repeated ten times. No shorter or additional trees were found at the end of this second round in any of the parsimony analyses. Three analyses were carried out under maximum parsimony, each with the settings specified above.

In the first analysis, all characters were treated as unordered and of equal unit weight. We obtained 23 shortest trees at 278 steps, with an ensemble consistency index of 0.5 (0.4908 excluding 5 parsimony-uninformative characters), an ensemble retention index of 0.6911 and an ensemble rescaled consistency index of 0.3456. A permutation-tail probability test⁵⁴ using 1,000 replicates showed that the length of the shortest trees differed significantly from random ($P < 0.001$). The strict consensus tree (Extended Data Fig. 7a) was poorly resolved. The Adams consensus tree (Extended Data Fig. 7b) had greater resolution, and placed *Parmastega* and *Elginerpeton* as the joint (unresolved) sister groups to all other tetrapods. The agreement subtree (a pruned topology that included only those taxa for which all most-parsimonious trees agreed upon mutual relationships) included 19 out of the 26 original taxa (Extended Data Fig. 7e): *Acanthostega*, *Dendrerpeton*, *Densignathus*, *Elginerpeton*, *Greererpeton*, *Ossinodus* and *Tantalognathus* were deleted. The node support value was evaluated via bootstrapping⁵⁵ and jackknifing⁵⁶ in PAUP*, in each case using 50% character resampling and 50,000

random resampling replicates with the fast step-wise addition. In both cases, very few nodes received support—namely post-*Panderichthys* taxa, post-elpistostegalian taxa, baphetids and a clade of *Eoherpeton* plus *Proterogyrinus*.

In the second analysis, characters were re-weighted by the largest values of their rescaled consistency indexes from the initial analysis. PAUP* yielded a single tree (Extended Data Fig. 7c) that was 112,3561 steps long, with an ensemble consistency index of 0.6804 (0.6655 excluding uninformative characters), an ensemble retention index of 0.8297 and an ensemble rescaled consistency index of 0.5645. This tree was three steps longer than the trees from the unweighted analysis and did not represent a significantly better fit for the data, in terms of tree length, than the unweighted trees (based upon Templeton, Kishino–Hasegawa, and winning-sites tests in PAUP*). The weighted analysis confirmed the status of *Parmastega* as the most-basal tetrapod.

In the third analysis, we used implied weighting⁵⁷, experimenting with different integer values for Goloboff’s constant of concavity K . We ran analyses with $1 \leq K \leq 10$ (for example, ref. ⁵⁸). For each K value, we saved all trees that were generated at the end of the analysis. The separate tree files obtained from all K -weighted analyses were stored in PAUP* after filtering out duplicated tree topologies. This process resulted in five K -weighted trees, which were summarized with a strict consensus (Extended Data Fig. 7f), an agreement subtree (Extended Data Fig. 7g) and an Adams consensus (Extended Data Fig. 7h). The agreement subtree included 22 taxa: *Densignathus*, *Elginerpeton*, *Metaxygnathus* and *Ossinodus* were deleted.

For the Bayesian inference analysis, we used MrBayes v. 3.2.6 (ref. ⁵⁹), with the following settings: variable coding; gamma-distributed rate model; 10⁷ generations and four chains; and discarding the first 25% of sampled trees. The convergence diagnostic was evaluated through inspection of the potential scale reduction factor values⁶⁰ output by MrBayes. These values approached or were identical to 1, indicating successfully convergent runs (Supplementary Information). Credibility values for nodes in the Bayesian results (Extended Data Fig. 7d) were moderate-to-strong for most nodes.

Reporting summary

Further information on research design is available in the Nature Research Reporting Summary linked to this paper.

Data availability

In total, 132 specimens comprising 183 skeletal elements were collected during the entire period of excavations (2002–2012). One hundred and six specimens (all of them figured in Supplementary Table 1) have been deposited in the collection of the Institute of Geology, Komi Science Centre (Ural Branch of the Russian Academy of Sciences, Syktyvkar, Russia) under collection number IG KSC 705/. One specimen has been deposited in the Ukhta Local Museum under collection number ULM 2599. The IG KSC and ULM specimens are available for examination. Other specimens have been reserved for sharing with other museums. The Life Science Identifier for *Parmastega* is urn:lsid:zoobank.org:act:76B5BB03-42FE-4F46-A284-F95E973CEE96.

- Chen, D. et al. A partial lower jaw of a tetrapod from “Romer’s Gap”. *Earth Env. Sci. Trans. R. Soc. Edinb.* **108**, 55–65 (2018).
- Wilkinson, M. Majority-rule reduced consensus trees and their use in bootstrapping. *Mol. Biol. Evol.* **13**, 437–444 (1996).
- Lloyd, G. T. Estimating morphological diversity and tempo with discrete character-taxon matrices: implementation, challenges, progress, and future directions. *Biol. J. Linn. Soc.* **118**, 131–151 (2016).
- Swofford, D. L. *PAUP* Phylogenetic Analysis Using Parsimony (*and Other Methods)* Version 4 (Sinauer, 2003).
- Wilkinson, M., Peres-Neto, P. R., Foster, P. G. & Moncrieff, C. B. Type 1 error rates of the parsimony permutation tail probability test. *Syst. Biol.* **51**, 524–527 (2002).
- Felsenstein, J. Confidence limits on phylogenies: an approach using the bootstrap. *Evolution* **39**, 783–791 (1985).

56. Farris, J. S., Albert, V. A., Källersjö, M., Lipscomb, D. & Kluge, A. G. Parsimony jackknifing outperforms neighbor-joining. *Cladistics* **12**, 99–124 (1996).
57. Goloboff, P. A. Estimating character weights during tree search. *Cladistics* **9**, 83–91 (1993).
58. Congreve, C. R. & Lamsdell, J. C. Implied weighting and its utility in palaeontological datasets: a study using modelled phylogenetic matrices. *Palaeontology* **59**, 447–462 (2016).
59. Ronquist, F. & Huelsenbeck, J. P. MrBayes 3: Bayesian phylogenetic inference under mixed models. *Bioinformatics* **19**, 1572–1574 (2003).
60. Gelman, A. & Rubin, D. B. Inference from iterative simulation using multiple sequences. *Stat. Sci.* **7**, 457–472 (1992).
61. Blom, H. Taxonomic revision of the Late Devonian tetrapod *Ichthyostega* from East Greenland. *Palaeontology* **48**, 111–134 (2005).
62. Ahlberg, P. E., Friedman, M. & Blom, H. New light on the earliest known tetrapod jaw. *J. Vertebr. Paleontol.* **25**, 720–724 (2005).
63. Robinson, J. The Evolution of the Early Tetrapod Middle Ear and Associated Structures. PhD thesis, Univ. College London (2006).

Acknowledgements We thank Y. Gatovsky, A. Zhuravlev and D. Ponomarev for their support of the project, and the dig crews of the 2009–2012 excavations for all their hard work. A. Ivanov identified the first tetrapod mandible from Sosnogorsk, in the Chernyshov Collection. P.A.B. acknowledges the support of National Geographic Society grant 9099-12 and UNDP/GEF

project no. 00059042. E.L. acknowledges the support of Latvian Council of Science grant Z-6153-110. P.E.A. acknowledges the support of a Wallenberg Scholarship from the Knut and Alice Wallenberg Foundation.

Author contributions P.A.B. initiated and directed the excavation programme at Sosnogorsk, which produced the material for the study. E.L. and P.E.A. participated in excavations. P.A.B. carried out all preparation, consolidation and photography of specimens. P.E.A. made the reconstructions of the skull, lower jaw and shoulder girdle. M.R. performed the phylogenetic analyses. P.E.A. made Figs. 1–3 and Extended Data Figs. 2, 4–9. P.A.B. made Extended Data Figs. 1, 3, as well as Supplementary Tables 1, 2. P.A.B., J.A.C., E.L., M.R. and P.E.A. participated in the interpretation of the material and the writing of the paper.

Competing interests The authors declare no competing interests.

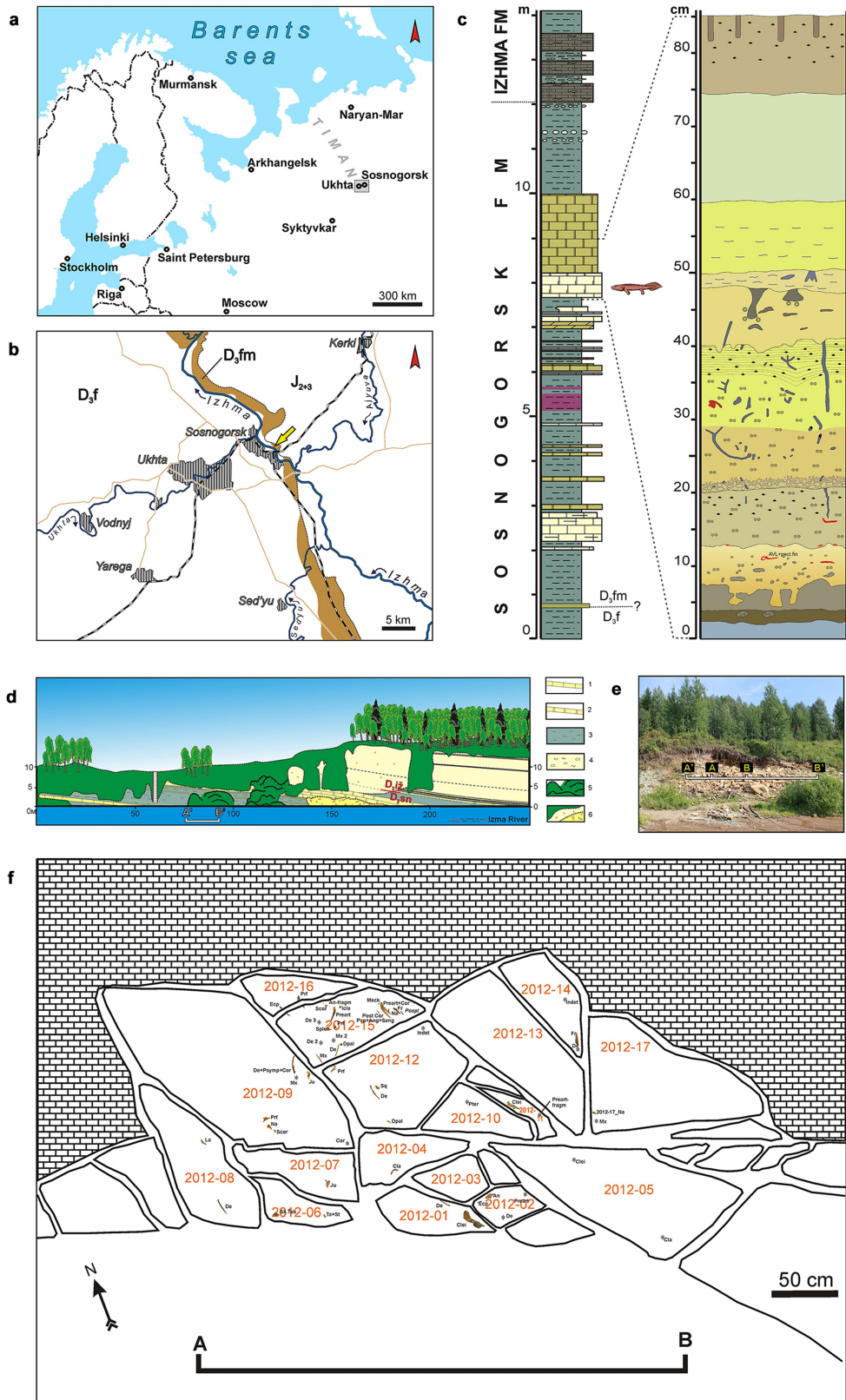
Additional information

Supplementary information is available for this paper at <https://doi.org/10.1038/s41586-019-1636-y>.

Correspondence and requests for materials should be addressed to P.E.A.

Peer review information *Nature* thanks Nadia Fröbisch and the other, anonymous, reviewer(s) for their contribution to the peer review of this work.

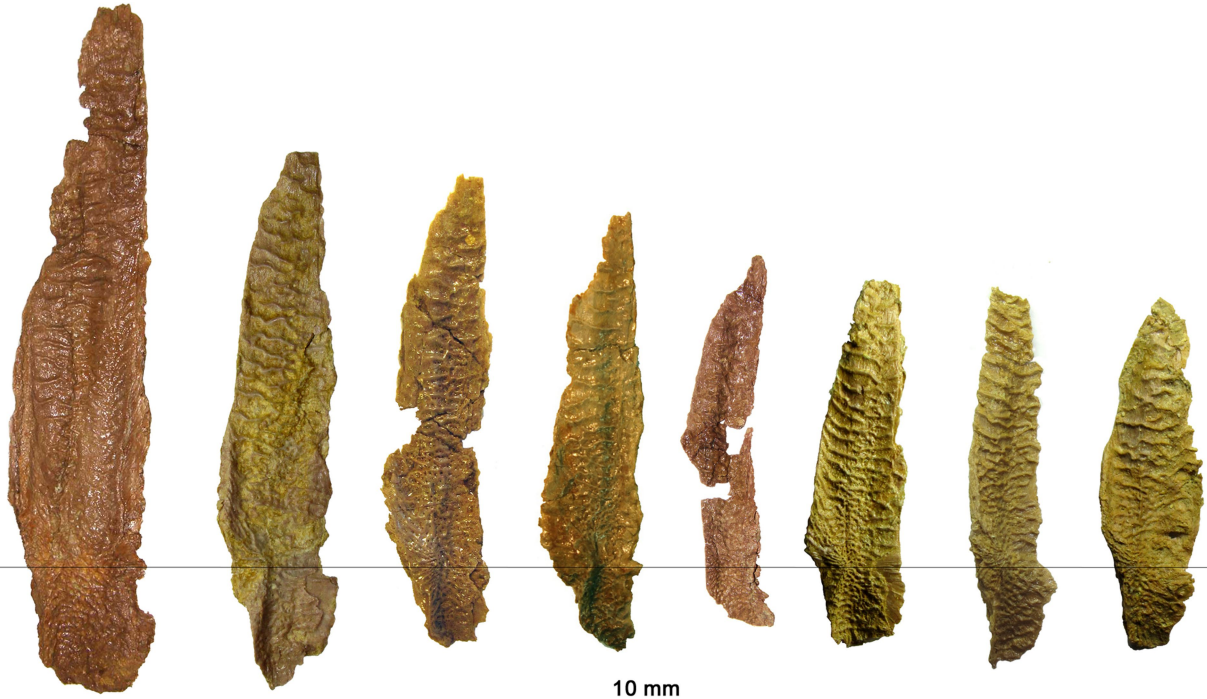
Reprints and permissions information is available at <http://www.nature.com/reprints>.



Extended Data Fig. 1 | See next page for caption.

Extended Data Fig. 1 | The distribution of *Parmastega* at the Sosnogorsk fossil site. a, b, Maps of increasing resolution, showing the location of Sosnogorsk within northwest Russia. The box around Ukhta and Sosnogorsk in **a** indicates the region shown in **b**. In **b**, the brown belt that extends from north to south indicates the outcrop of Famennian (D_3fm) deposits in the region, and the yellow arrow points to the Sosnogorsk fossil site (Sosnovskiy Geological Monument). **c**, Stratigraphic column through the Sosnogorsk Formation, and part of the overlying marine Izhma Formation. Note the possible position of the Frasnian–Famennian boundary (D_3f – D_3fm) in the lower part of the Sosnogorsk Formation. The vertebrate-bearing part of the formation is shown in detail on the right; the tetrapod-bearing level is indicated with a red vertical bar.

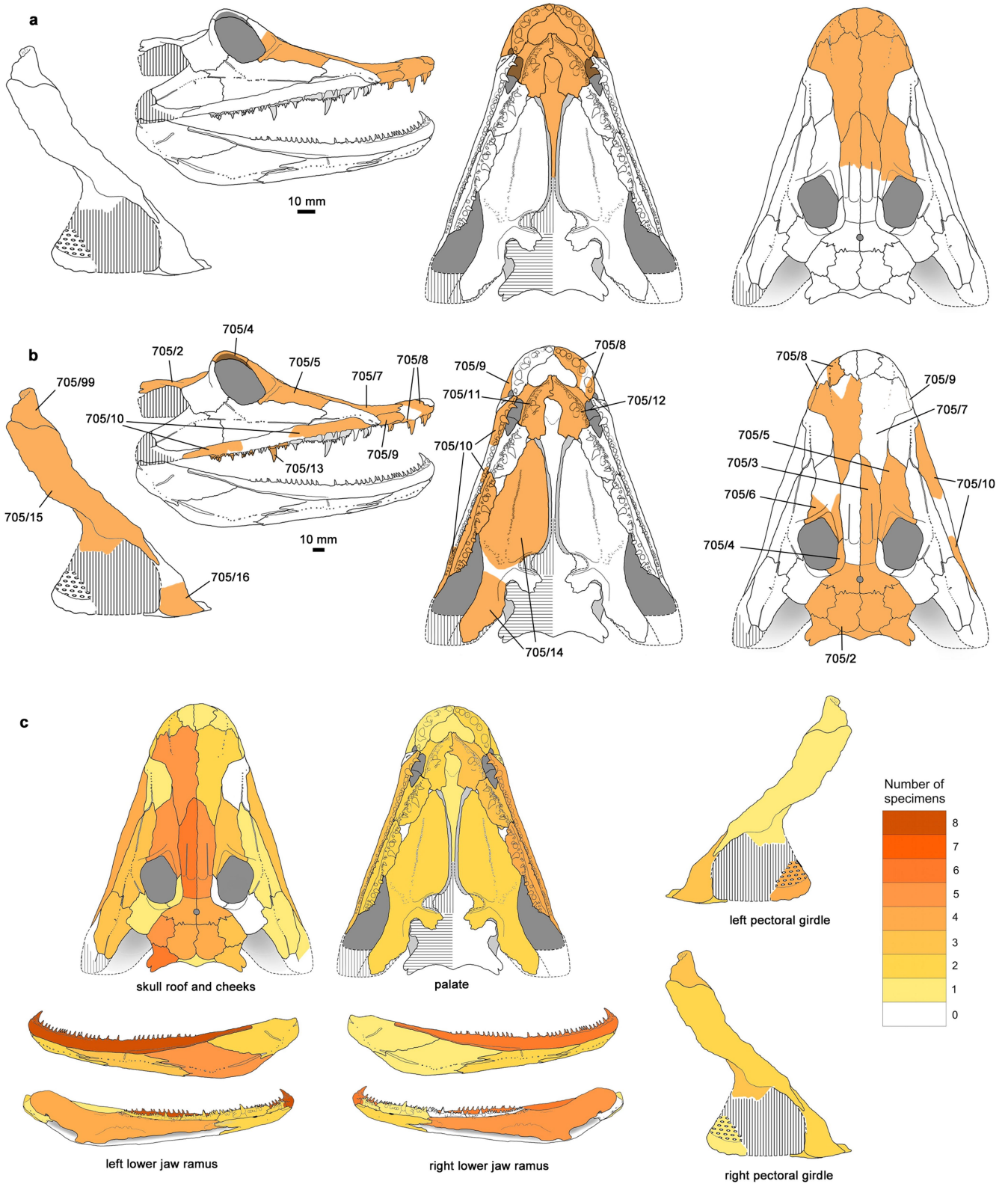
d, General view of outcrop no. 20 (Sosnovskiy Geological Monument) from the opposite bank of the Izhma River. 1, limestone; 2, dolomite; 3, clay; 4, nodular limestone; 5, scree; and 6, landslide. D_3sn , Sosnogorsk Formation, D_3iz , Izhma Formation. The distance A–B' indicates the area of the main excavation that took place in 2010–2012. **e**, Main excavation. The distance A–B indicates the area in which all of the tetrapod bones were found, during the excavation in 2012. The photograph was taken on 2 August 2012. **f**, Sketch map of the main excavation (2012), showing the distribution of tetrapod bones within the bed. The cluster numbers are indicated in orange. The background maps in **a** and **b** were taken from <https://yandex.ru/maps>; the geological features of **b** were taken from the open-access State Geological Map at <https://vsegei.ru/>.



Extended Data Fig. 2 | Frontal bones of *Parmastega*. This figure shows all of the complete and near-complete frontals of *Parmastega* (eight out of nine known frontals) to scale, oriented with anterior at the top and aligned on the centre of radiation (horizontal line). The right frontals have been reversed so

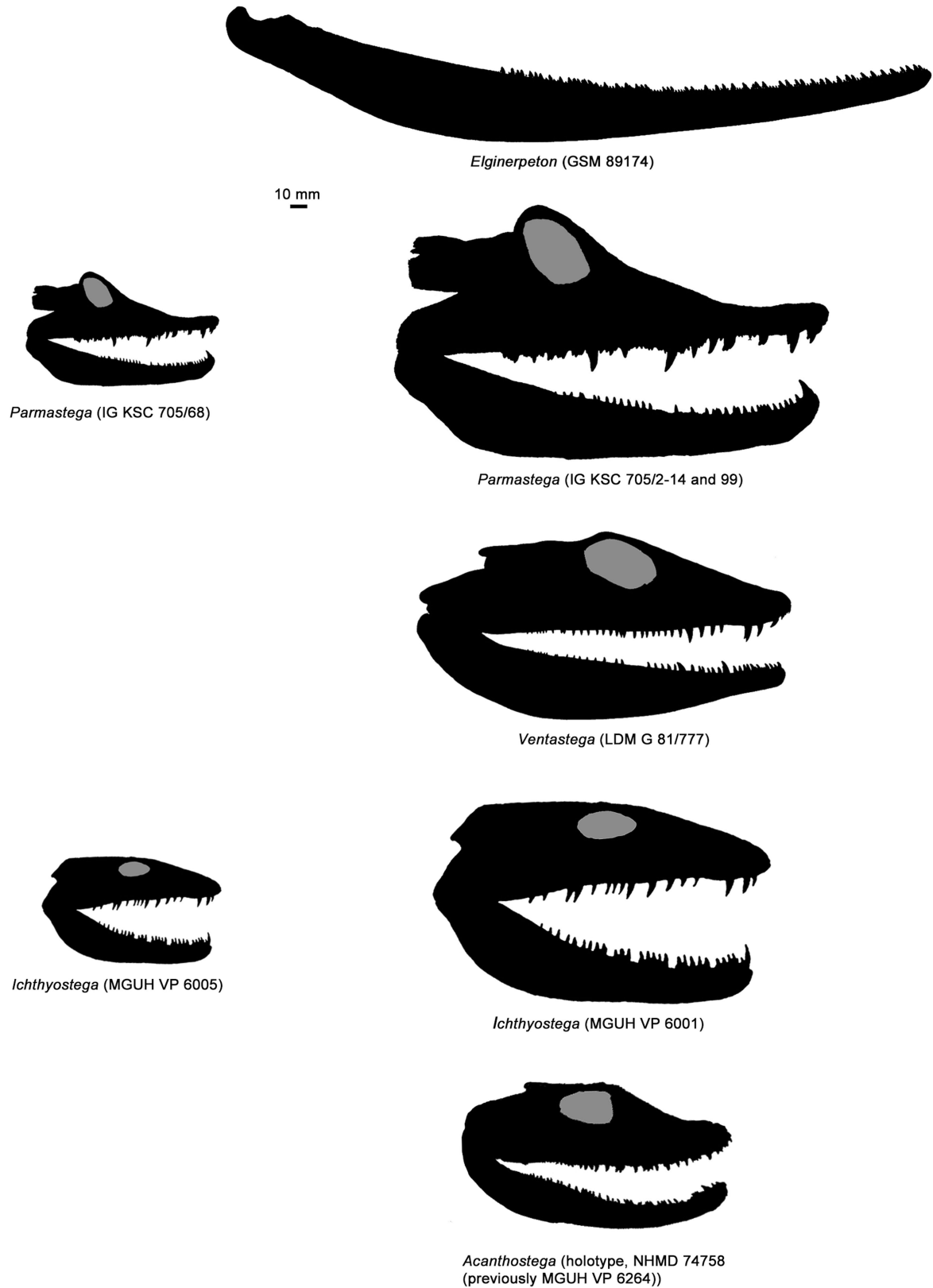
10 mm

that all bones have the appearance of left frontals. From left to right, the specimens are IG KSC 705/3 (reversed), IG KSC 705/40, IG KSC 705/44 (reversed), IG KSC 705/43, IG KSC 705/45, IG KSC 705/18 (reversed), IG KSC 705/42 and IG KSC 705/41. Scale bar, 10 mm.



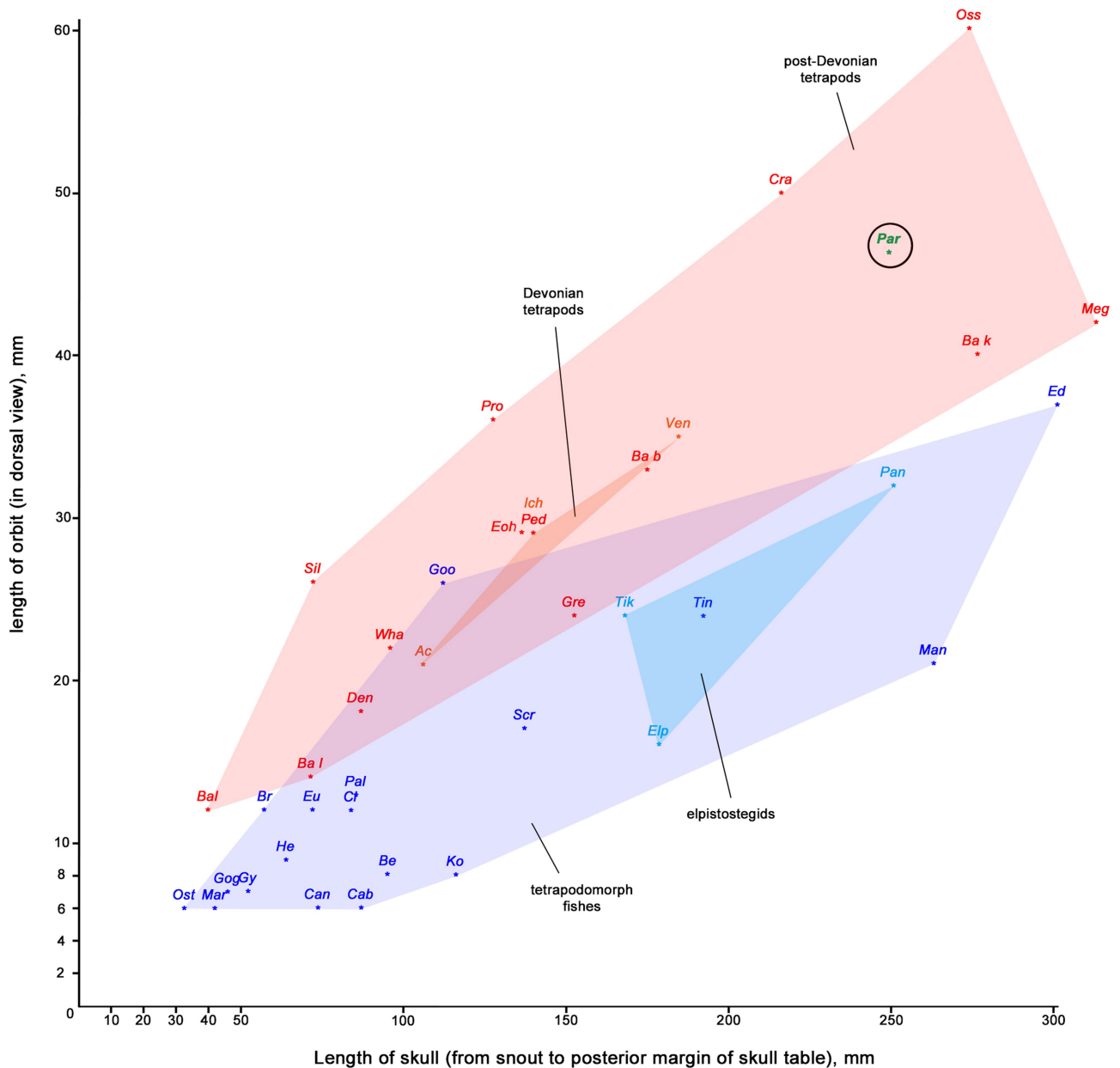
Extended Data Fig. 3 | Bone associations. **a, b,** Diagrammatic images showing the associated bones (in orange) of two individual skulls. **a,** The holotype IGKSC 705/1. **b,** The largest individual, IGKSC 705/2-705/14 and IGKSC 705/99.

In the lateral view of **b,** the preserved frontal and nasal are shown (even though they are in fact on the other side of the skull). **c,** Diagrammatic representation of the number of specimens of different bones in the sample.



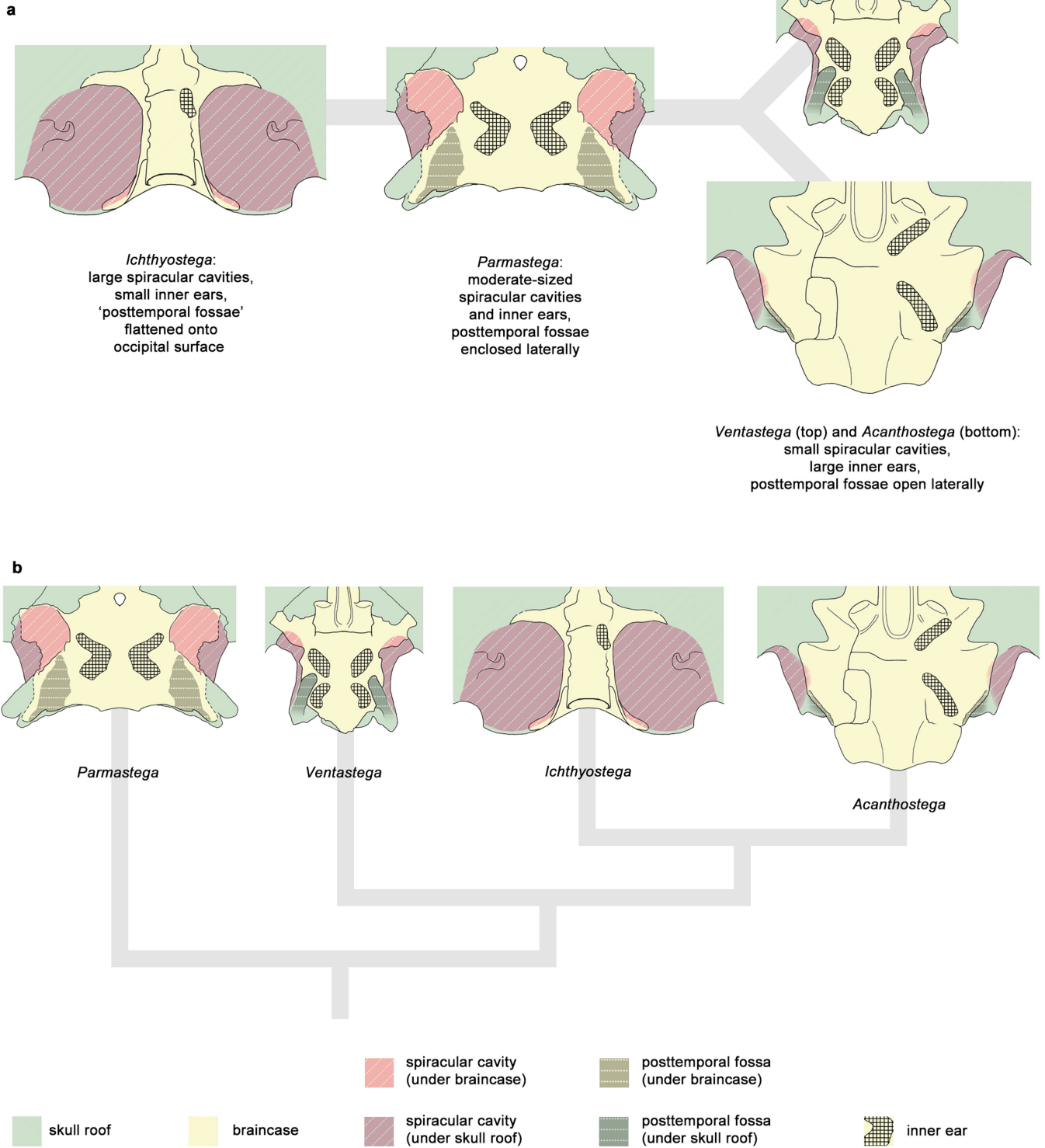
Extended Data Fig. 4 | Size and shape of Devonian tetrapods. Silhouette reconstructions of the heads of known, reconstructable Devonian tetrapods. Reconstructions are drawn to the same scale. The lower jaw of *Elginerpeton*—the largest known Devonian tetrapod, and for which the skull cannot be reconstructed—is also included. All reconstructions except for *Acanthostega* are assembled from more than one specimen; the specimen numbers indicate the specimen used to determine the scale. The right-hand column shows the largest

known individuals. The left-hand column shows the smallest individuals of *Parmastega* (all from Sosnogorsk) and *Ichthyostega* (based on the entire East Greenland collection, reviewed in ref.⁶⁴). Note the similarity in size range despite the very different nature of the samples. *Ventastega* and *Acanthostega* show narrow size ranges, which are not illustrated. Reconstructions modified from the following sources: *Ichthyostega*, ref.¹⁹; *Acanthostega*, ref.³¹; *Ventastega*, ref.³²; *Elginerpeton*, ref.⁶².



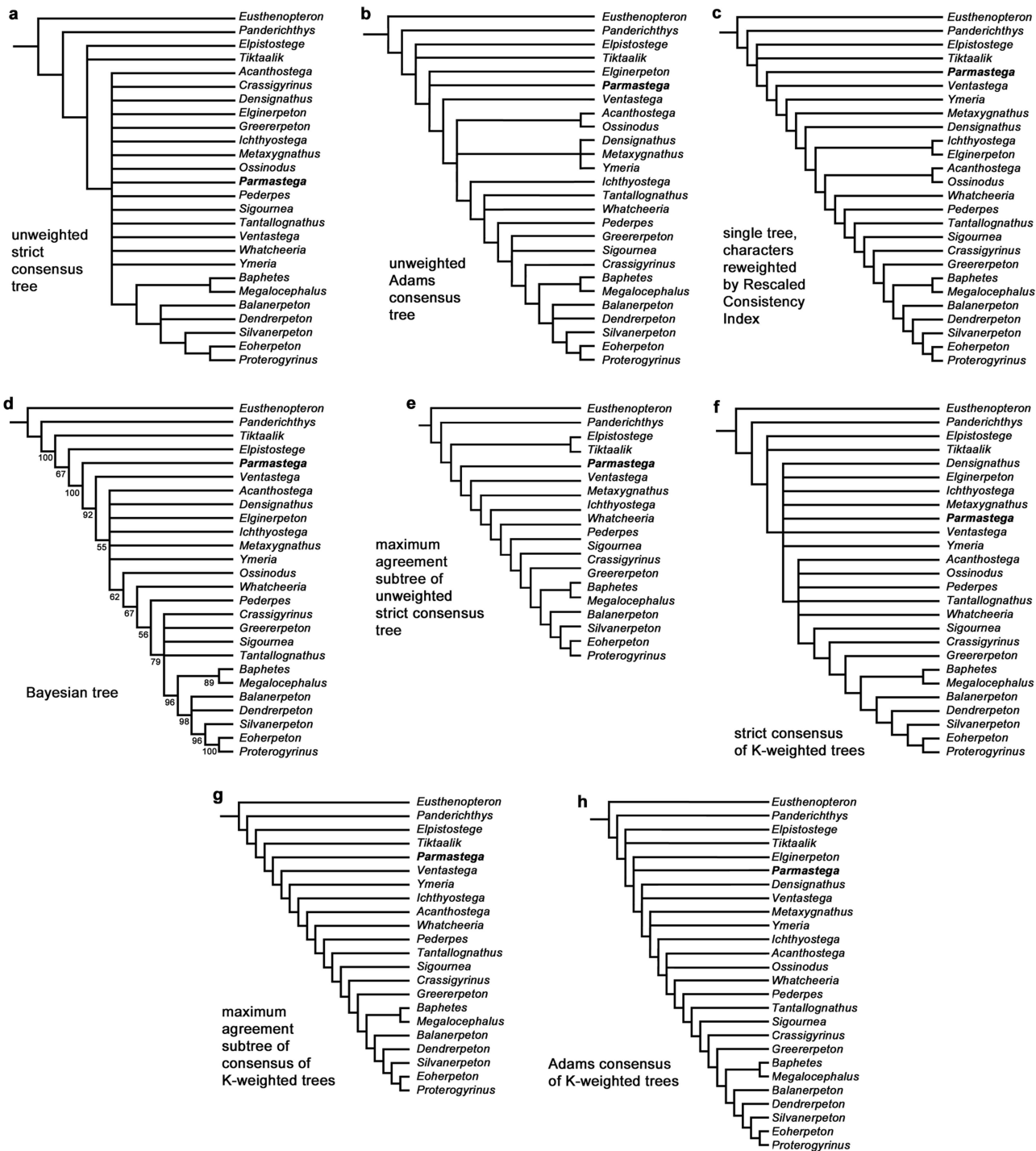
Extended Data Fig. 5 | Relative orbit size. Plot of orbit length versus skull length for a range of tetrapodomorph fishes, elpistostegids, Devonian tetrapods and post-Devonian tetrapods. Data are taken from ref. ⁴⁷, except *Parmastega*, which is based on the largest known individual (Extended Data Fig. 3). Post-Devonian tetrapods from ref. ⁴⁷ not included in our phylogenetic analysis are not shown. *Ac*, *Acanthostega*; *Ba b*, *Baphetes bohemicus*; *Ba k*, *Baphetes kirkbyi*; *Ba l*, *Baphetes lintonensis*; *Bal*, *Balanerpeton*; *Be*, *Beelarongia*; *Br*, *Bruehnopteron*; *Cab*, *Cabonnichthys*; *Can*, *Canowindra*; *Cl*, *Cladrosymblema*;

Cra, *Crassigyrynus*; *Den*, *Dendrerpeton*; *Ed*, *Edenopteron*; *Elp*, *Elpistostege*; *Eoh*, *Eoherpeton*; *Eu*, *Eusthenopteron*; *Gog*, *Gogonassus*; *Goo*, *Gooloogongia*; *Gre*, *Greererpeton*; *Gy*, *Gyroptychius*; *He*, *Heddeleithys*; *Ich*, *Ichthyostega*; *Ko*, *Koharalepis*; *Man*, *Mandageria*; *Mar*, *Marsdenichthys*; *Meg*, *Megalocephalus*; *Oss*, *Ossinodus*; *Ost*, *Osteolepis*; *Pal*, *Palatinichthys*; *Pan*, *Panderichthys*; *Par*, *Parmastega*; *Ped*, *Pederpes*; *Pro*, *Proterogyrynus*; *Scr*, *Screbinodus*; *Sil*, *Silvanerpeton*; *Tik*, *Tiktaalik*; *Tin*, *Tinirau*; *Ven*, *Ventastega*; *Wha*, *Whatcheeria*.



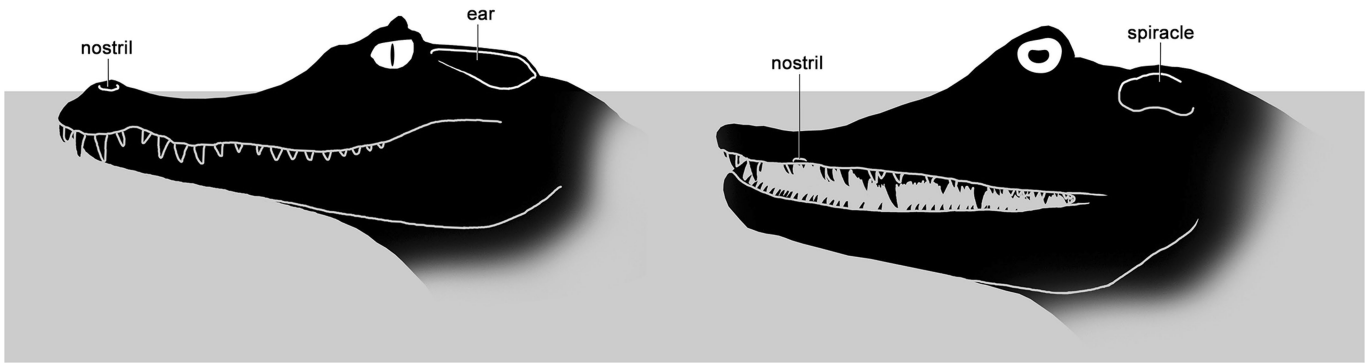
Extended Data Fig. 6 | Otoccipital morphologies of Devonian tetrapods. a, Comparative diagram of the otoccipital regions of *Parmastega*, *Ichthyostega* (new reconstruction, based on data from refs. ^{18,20}), *Ventastega* (modified from ref. ³²) and *Acanthostega* (modified from ref. ²⁰, semicircular canals modified from ref. ⁶³) in ventral view. The basioccipital–exoccipital complex is preserved only in *Ichthyostega* and *Acanthostega*; in these genera the inner ear is shown only on one side. Drawings are scaled to the same length from pineal region to

posterior margin of otic capsule. The inner ear is represented by the grooves for the anterior and posterior oblique semicircular canals, except in *Ichthyostega* in which it is represented by the sacculus (modified from ref. ²⁰). The braincases are arranged by morphological similarity, so that a minimum number of transformations are required along each branch. **b,** Consensus phylogeny from the analyses presented in this paper. The phylogenetic topology does not match the similarity dendrogram.



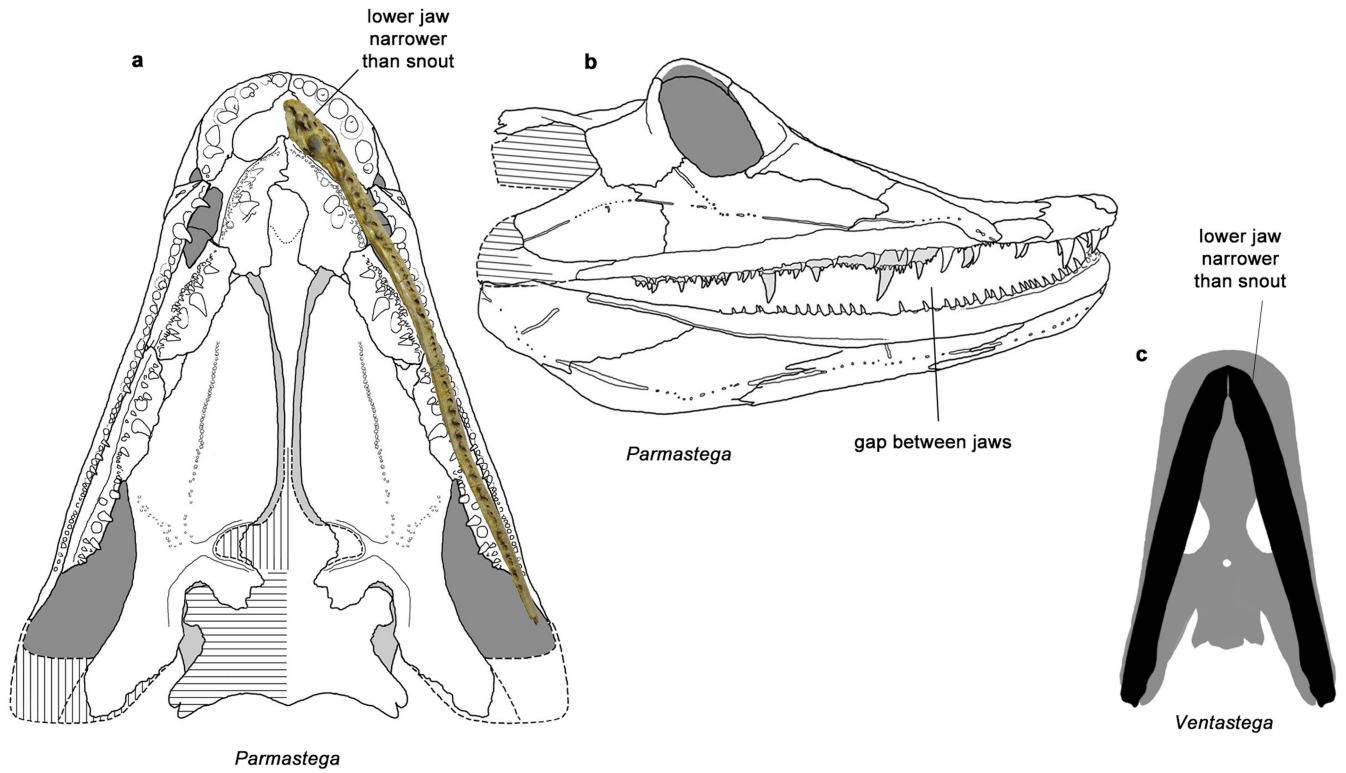
Extended Data Fig. 7 | Phylogenetic analysis. **a**, Unweighted strict-consensus tree. **b**, Unweighted Adams consensus tree. **c**, Single tree resulting from reweighting characters by the rescaled consistency index. **d**, Bayesian tree, with credibility values at nodes. **e**, Maximum-agreement subtree of unweighted

parsimony analysis. **f**, Strict consensus of K -weighted trees. **g**, Maximum-agreement subtree of K -weighted parsimony analysis. **h**, Adams consensus of all trees from all K -weighted analyses.



Extended Data Fig. 8 | *Parmastega* and caiman. Comparison in left lateral view of spectacled caiman (*Caiman crocodilus*) on the left and *Parmastega* on the right, drawn to the same size, showing the inferred similar cruising posture at

the surface. Note the difference in the positions of the nostrils. The caiman image is based on a computed tomography scan of a skull in the Digimorph Archive (http://www.digimorph.org/specimens/Caiman_crocodilus/).



Extended Data Fig. 9 | Fit of dentary against upper jaw. a, Dentary of *Parmastega* (IG KSC 705-67) fitted against palatal reconstruction to show the difference in curvature between the spade-shaped snout and the relatively straight dentary. **b,** Lateral view of skull reconstruction of *Parmastega* with

closed mouth, showing mismatch in curvature between upper and lower jaws. **c,** Composite reconstruction of *Ventastega*, superimposing lower jaw rami (from ref. ³⁰) on skull reconstruction (from ref. ³²), showing shape relationship similar to a. Not to scale.

Reporting Summary

Nature Research wishes to improve the reproducibility of the work that we publish. This form provides structure for consistency and transparency in reporting. For further information on Nature Research policies, see [Authors & Referees](#) and the [Editorial Policy Checklist](#).

Statistics

For all statistical analyses, confirm that the following items are present in the figure legend, table legend, main text, or Methods section.

n/a Confirmed

- The exact sample size (n) for each experimental group/condition, given as a discrete number and unit of measurement
- A statement on whether measurements were taken from distinct samples or whether the same sample was measured repeatedly
- The statistical test(s) used AND whether they are one- or two-sided
Only common tests should be described solely by name; describe more complex techniques in the Methods section.
- A description of all covariates tested
- A description of any assumptions or corrections, such as tests of normality and adjustment for multiple comparisons
- A full description of the statistical parameters including central tendency (e.g. means) or other basic estimates (e.g. regression coefficient) AND variation (e.g. standard deviation) or associated estimates of uncertainty (e.g. confidence intervals)
- For null hypothesis testing, the test statistic (e.g. F , t , r) with confidence intervals, effect sizes, degrees of freedom and P value noted
Give P values as exact values whenever suitable.
- For Bayesian analysis, information on the choice of priors and Markov chain Monte Carlo settings
- For hierarchical and complex designs, identification of the appropriate level for tests and full reporting of outcomes
- Estimates of effect sizes (e.g. Cohen's d , Pearson's r), indicating how they were calculated

Our web collection on [statistics for biologists](#) contains articles on many of the points above.

Software and code

Policy information about [availability of computer code](#)

Data collection

Materialise 3-matic Research 12.0 (software for manipulating three-dimensional virtual objects in space; used for constructing model of pectoral girdle of *Parmastega*).

Data analysis

PAUP* version 4.0a and MrBayes version 3.2.6 (for phylogenetic analysis)

For manuscripts utilizing custom algorithms or software that are central to the research but not yet described in published literature, software must be made available to editors/reviewers. We strongly encourage code deposition in a community repository (e.g. GitHub). See the Nature Research [guidelines for submitting code & software](#) for further information.

Data

Policy information about [availability of data](#)

All manuscripts must include a [data availability statement](#). This statement should provide the following information, where applicable:

- Accession codes, unique identifiers, or web links for publicly available datasets
- A list of figures that have associated raw data
- A description of any restrictions on data availability

All specimens figured and described in the paper are accessioned to the Institute of Geology, Komi Science Centre, Ural Branch of the Russian Academy of Sciences, Syktyvkar, Russia, and are deposited there. The accession code is IG KSC 705/. All the specimens are available for examination.

Field-specific reporting

Please select the one below that is the best fit for your research. If you are not sure, read the appropriate sections before making your selection.

Life sciences Behavioural & social sciences Ecological, evolutionary & environmental sciences

For a reference copy of the document with all sections, see [nature.com/documents/nr-reporting-summary-flat.pdf](https://www.nature.com/documents/nr-reporting-summary-flat.pdf)

Ecological, evolutionary & environmental sciences study design

All studies must disclose on these points even when the disclosure is negative.

Study description	Description of fossil material of the Devonian tetrapod <i>Parmastega aelidae</i> .
Research sample	All known specimens of this taxon.
Sampling strategy	We excavated the fossil locality (Sosnovskiy Geological Monument, at Sosnogorsk on the bank of the Izhma River) and collected all the fossils we could find. The fossils were freed from the rock with dilute acetic acid by Pavel Beznosov.
Data collection	The primary interpretation of the fossils and the assembly of the reconstruction were undertaken by Pavel Beznosov and Per Ahlberg, working with the specimens in Syktyvkar during a series of visits by Per Ahlberg.
Timing and spatial scale	Excavations were carried out during 2002-2012.
Data exclusions	No data were excluded.
Reproducibility	Not applicable.
Randomization	Not applicable.
Blinding	Not applicable.
Did the study involve field work?	<input checked="" type="checkbox"/> Yes <input type="checkbox"/> No

Field work, collection and transport

Field conditions	Typical summer weather in northern Russia. The weather conditions had no impact on data gathering.
Location	Sosnovskiy Geological Monument, Sosnogorsk, right bank of Izhma River, Komi Republic, Russia.
Access and import/export	The fieldwork was carried out by the Geological Institute of the Komi Science Center, Uralian Branch of the Russian Academy of Sciences, in accordance with local and national regulations. The material was not exported from Russia.
Disturbance	Blocks of limestone were removed from the riverbank. The annual ice-melt and spring flood of the Izhma River vigorously scours the banks and soon removes any trace of human disturbance.

Reporting for specific materials, systems and methods

We require information from authors about some types of materials, experimental systems and methods used in many studies. Here, indicate whether each material, system or method listed is relevant to your study. If you are not sure if a list item applies to your research, read the appropriate section before selecting a response.

Materials & experimental systems

n/a	Included in the study
<input checked="" type="checkbox"/>	<input type="checkbox"/> Antibodies
<input checked="" type="checkbox"/>	<input type="checkbox"/> Eukaryotic cell lines
<input type="checkbox"/>	<input checked="" type="checkbox"/> Palaeontology
<input checked="" type="checkbox"/>	<input type="checkbox"/> Animals and other organisms
<input checked="" type="checkbox"/>	<input type="checkbox"/> Human research participants
<input checked="" type="checkbox"/>	<input type="checkbox"/> Clinical data

Methods

n/a	Included in the study
<input checked="" type="checkbox"/>	<input type="checkbox"/> ChIP-seq
<input checked="" type="checkbox"/>	<input type="checkbox"/> Flow cytometry
<input checked="" type="checkbox"/>	<input type="checkbox"/> MRI-based neuroimaging

Palaeontology

Specimen provenance

The specimens come from the Sosnovskiy Geological Monument, Sosnogorsk, right bank of Izhma River, Komi Republic, Russia, and were collected by the Geological Institute of the Komi Science Center, Uralian Branch of the Russian Academy of Sciences in accordance with local and national regulations.

Specimen deposition

Geological Institute of the Komi Science Center, Uralian Branch of the Russian Academy of Sciences

Dating methods

Not applicable

Tick this box to confirm that the raw and calibrated dates are available in the paper or in Supplementary Information.